Geometrical Isomerism of the Exocyclic C=C Bonds of Heptafulvene Derivatives. Steric and Electronic Effects on the Rotational Barrier

Yukari Ikeda, Bing Zhu Yin, Nobuo Kato, Akira Mori, and Hitoshi Takeshita[*]
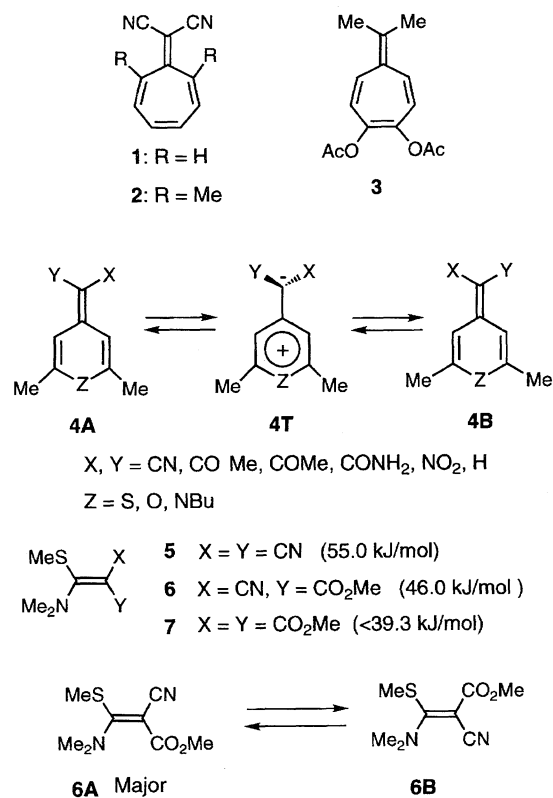
Institute of Advanced Material Study, 86, Kyushu University, Kasuga-koen, Kasuga, Fukuoka 816

(Received October 30, 1995)

The rotational barriers of the exocyclic double bonds of a series of methyl 8-cyanoheptafulvene-8-carboxylates were measured to evaluate the steric effect and the contribution of the polarized structures. An incorporation of five-membered heterocycles lowered the activation energies sufficiently to allow the study of steric and electronic factors. Thus, the Type I compounds, 8-[cyano(methoxycarbonyl)methylidene]-2-methyl-8*H*-cyclohepta[*b*]furan and its sulfur and nitrogen analogues, which have a different extent of steric effect, had rates of rotation in the order of N>S>O. On the other hand, the Type II derivatives, 6-(1-cyano-1-methoxycarbonylmethylidene)-2-methylcyclohepta[*b*]furan and its sulfur and nitrogen analogues, for which the steric factor is unimportant, showed an order of N>O>S. This was also the case for the Type III derivatives, methyl 8-cyano-3-methoxyheptafulvene-8-carboxylate, methyl 8-cyano-3-(methylthio)heptafulvene-8-carboxylate, and methyl 8-cyano-3-(dimethylamino)heptafulvene-8-carboxylate. The unusually low values of $\Delta H^{\ddagger}$ for the nitrogen analogues indicated that the ground state structures were destabilized by the steric repulsions.

Heptafulvenes, fundamental members of non-alternant conjugated compounds, can be promising compounds for functional uses in view of their peculiar conjugated π structure. The lengths of the exocyclic C=C bonds of the heptafulvenes have been discussed as a measure of the contribution of a dipolar form.[1] The substituents on the exocyclic C=C bond affect the chemical and physical properties of heptafulvenes. According to the X-ray crystallographic analysis, the seven-membered ring of 8,8-dicyanoheptafulvene (**1**) is nearly planar,[1] but the rings of 8,8-dicyano-1,6-dimethylheptafulvene (**2**)[2] and 3,4-diacetoxy-8,8-dimethyl-heptafulvene (**3**) are puckered.[3] Furthermore, the exocyclic C=C bond length of **1** is 1.42 Å, having a considerable single bond character,[1] whereas that of **3** is 1.343 Å, a typical length for normal C=C bonds.[3] This was explained in terms of the different dipolar contributions to the structure of these molecules.

Another measure of the dipolar contributions should be the rates of rotation about the polarized C=C bond, which could be determined with variable-temperature NMR techniques. The thermodynamic analysis of 4-methylidene (with electron-withdrawing substituents) derivatives (**4**) of 4*H*-pyran, 4*H*-thiopyran, and 1,4-dihydropyridine, to be designated as "push-pull" ethene systems, showed that **4A** (*E*-form) isomerized to the isomers **4B** (*Z*-form) via the dipolar transition state **4T**.[4,5] The rates showed a decreasing order of N>S>O. The C=C bond length[6] and the barrier[7] to rotation about the C=C bond of a push–pull ethene, [dimethylamino-(methylthio)methylidene]malononitrile (**5**), were shown to be 1.397 Å and 55.0 kJ mol^{-1}. The replacement of the cyano group in **5** by a methoxycarbonyl group decreased the

1: R = H
2: R = Me

3

X, Y = CN, CO Me, COMe, CONH$_2$, NO$_2$, H
Z = S, O, NBu

4A   **4T**   **4B**

5   X = Y = CN   (55.0 kJ/mol)
6   X = CN, Y = CO$_2$Me   (46.0 kJ/mol)
7   X = Y = CO$_2$Me   (<39.3 kJ/mol)

6A Major   **6B**

Scheme 1.

rotational barrier (**6**, 46.0 kJ mol^{-1} in dichloromethane, and **7**, 39.3 kJ mol^{-1} in dichloromethane and 37.2 kJ mol^{-1} in acetone).[8] Thus, rotational barriers of the C=C bond were

1320 *Bull. Chem. Soc. Jpn.*, **69**, No. 5 *(1996)*

Geometrical Isomerism of Heptafulvenes

sensitive to structural variations.[9] In this paper, we discuss the dynamic behavior of three types of heptafulvenes;[10,11] heterocycle-fused push–pull heptafulvenes, 8-[cyano(methoxycarbonyl)methylidene]-2-methyl-8*H*-cyclohepta[*b*]furan and its sulfur and nitrogen analogues (**8**, **9**, and **10**) (Type I), 6-[cyano(methoxycarbonyl)methylidene]-2-methyl-6*H*-cyclohepta[*b*]furan and its sulfur and nitrogen analogues (**11**, **12**, and **13**) (Type II), and monocyclic heptafulvenes, methyl 8-cyano-3-methoxyheptafulvene-8-carboxylate (**14**), methyl 8-cyano-3-(methylthio)heptafulvene-8-carboxylate (**15**), and methyl 8-cyano-3-(dimethylamino)heptafulvene-8-carboxylate (**16**) (Type III). We analyze the electronic and steric effects of the hetero atoms on the rotation about the exocyclic C=C bond, together with four isopropyl derivatives (**18**—**21**) of **9**.

Experimental

Measurement of Temperature. Accuracy of temperature measurement, ca. ±0.9 °C, under the non-irradiating conditions was confirmed by careful thermocouple calibration by Mr. Kohji Hamano, of Institute of Advanced Material Study, Kyushu University, to whom our thanks are due. Accordingly, we have discarded the subdecimal figures of the displays.

Materials. Methyl 8-cyanoheptafulvene-8-carboxylates were prepared from corresponding tropone precursors[12,13] and methyl cyanoacetate by refluxing in acetic anhydride. In Chart 1, the compounds are illustrated with the reference sources. Physical constants, including the NMR data measured in chloroform-*d* at room temperature, of characterized new compounds are listed below, and the yields from troponic precursors are shown in brackets:

17(11%): Red prisms, mp 129—130 °C (AcOEt–hexane); ^{1}H NMR δ = 3.81 (3H, s), 6.82—7.02 (3H, m), 6.95 (1H, dd, J = 11.5, 7.7 Hz), 7.47 (1H, dm, J = 11.5 Hz), 8.72 (1H, dm, J = 10.3 Hz); ^{13}C NMR δ = 52.1, 89.8, 118.4, 134.9, 136.5, 137.1, 137.3, 137.5, 138.3, 161.5, 164.7; IR (KBr) 2192, 1696, 1629, 1520, 1494, 1425, 1401, 1261, 1222, 1178, 1118, 1019, 830, 777 cm^{-1}; UV λ_{max}^{MeOH} = 255 nm (ε 11100), 389 (21700), 403 (19600 sh); *m/z* 187 (M$^+$; 94), 156 (100), 128 (24), 101 (25), 77 (24), 51 (18). Found: C, 70.80; H, 4.98; N, 7.32%. Calcd for C$_{11}$H$_9$NO$_2$: C, 70.58; H, 4.85; N, 7.48%.

18(72%): Reddish-orange prisms, mp 124—126 °C (AcOEt–cyclohexane); ^{1}H NMR δ = 1.27 (6H, d, J = 7.0 Hz), 2.59 (3H, d, J = 1.1 Hz), 3.21 (1H, sept, J = 7.0 Hz), 3.84 (3H, s), 6.69 (1H, dm, J = 8.1 Hz), 6.83 (1H, dd, J = 11.0, 8.1 Hz), 7.21 (1H, q, J = 1.1 Hz), 8.17 (1H, br d, J = 11.0 Hz); ^{13}C NMR δ = 15.7, 23.3 (2C), 34.3, 52.3, 90.1, 119.6, 124.5, 125.6, 126.1, 132.4, 135.6, 144.4, 145.5, 152.0, 157.3, 164.3; IR (KBr) 2964, 2194, 1700, 1615, 1572, 1488, 1423, 1316, 1239, 1212, 1125, 1049, 906, 846, 792 cm^{-1}; UV λ_{max}^{MeOH} = 206 nm (ε 14800), 256 (9250), 282 (5700 sh), 423

(10800); *m/z* 299 (M$^+$; 100), 284 (11), 268 (16), 256 (33), 59 (5). Found: C, 68.23; H, 5.75; N, 4.39%. Calcd for C$_{17}$H$_{17}$NO$_2$S: C, 68.20; H, 5.72; N, 4.68%.

19(50%): Red prisms, mp 97—98 °C (AcOEt–hexane); ^{1}H NMR δ = 1.24 (6H, d, J = 7.0 Hz), 2.58 (3H, d, J = 0.7 Hz), 2.77 (1H, sept, J = 7.0 Hz), 3.84 (3H, s), 6.89 (1H, dd, J = 12.6, 1.8 Hz), 6.97 (1H, q, J = 0.7 Hz), 7.25 (1H, d, J = 1.8 Hz), 8.53 (1H, br, J = 12.6 Hz); ^{13}C NMR δ = 15.6, 22.9 (2C), 36.8, 52.3, 87.4, 120.5, 127.7, 128.4, 129.6, 134.8, 135.9, 145.9, 146.5, 150.1, 156.3, 165.2; IR (KBr) 2958, 2188, 1686, 1560, 1500, 1410, 1333, 1314, 1231, 1183, 1120, 1072, 902, 849, 765, 666 cm^{-1}; UV λ_{max}^{MeOH} = 208 nm (ε 21100), 255 (16600), 268 (15000 sh), 344 (5200), 430 (17500); *m/z* 299 (M$^+$; 100), 268 (25), 256 (14). Found: C, 68.49; H, 5.72; N, 4.59%. Calcd for C$_{17}$H$_{17}$NO$_2$S: C, 68.20; H, 5.72; N, 4.68%.

20(11%): A red oil; ^{1}H NMR δ = 1.25 (6H, d, J = 7.0 Hz), 2.58 (3H, d, J = 0.7 Hz), 2.82 (1H, sept, J = 7.0 Hz), 3.84 (3H, s), 6.78 (1H, dd, J = 11.3, 1.8 Hz), 6.97 (1H, q, J = 0.7 Hz), 7.32 (1H, d, J = 11.3 Hz), 8.48 (1H, br s); ^{13}C NMR δ = 15.2, 23.0 (2C), 38.8, 52.2, 87.8, 120.6, 124.8, 128.9, 131.2, 131.6, 137.2, 145.2, 145.5, 154.2, 157.1, 165.2; IR (neat) 2962, 2194, 1701, 1625, 1564, 1525, 1450, 1377, 1325, 1227, 1108, 912, 848, 755 cm^{-1}; UV λ_{max}^{MeOH} = 206 nm (ε 20200), 272 (14400), 342 (5400), 420 (14200); *m/z* 299 (M$^+$; 100), 268 (22), 256 (17), 43 (7). Found: *m/z* 299.0979 (M$^+$). Calcd for C$_{17}$H$_{17}$NO$_2$S: M, 299.0979.

22(83%): Yellow needles, mp 217—218 °C; ^{1}H NMR δ = 2.56 (3H, d, J = 1.0 Hz), 6.28 (1H, q, J = 1.0 Hz), 6.87 (1H, ddd, J = 10.0, 8.0, 1.5 Hz), 7.06 (1H, ddd, J = 12.0, 8.0, 2.0 Hz), 7.26 (1H, m), 7.52 (1H, m); ^{13}C NMR δ = 14.0, 61.5, 110.4, 116.4 (2C), 130.9, 131.1, 131.8, 135.7, 136.3, 148.8, 149.8, 159.9; IR (KBr) 2200 cm^{-1}; MS *m/z* (rel intensity) 209 (M$^+$+1; 15), 208 (M$^+$; 100), 153 (12). Found: C, 74.77; H, 4.02; N, 13.63%. Anal. Calcd for C$_{13}$H$_8$N$_2$O: C, 74.98; H, 3.88; N, 13.46%.

23(45%): Yellow needles, mp 220—221 °C; ^{1}H NMR δ = 2.63 (3H, d, J = 1.0 Hz), 6.80 (1H, ddd, J = 10.0, 8.0, 1.5 Hz), 6.99 (1H, ddd, J = 12.0, 8.0, 2.0 Hz), 7.04 (1H, q, J = 1.0 Hz), 7.3—7.5 (2H, m); ^{13}C NMR δ = 15.7, 66.5, 116.2, 117.2, 129.7, 130.0, 131.0, 134.3, 136.4, 138.3, 146.8, 148.0, 157.0; IR (KBr) 2200 cm^{-1}; UV (MeOH) 250.4 nm (ε 18400), 269.0 (19600), 313.8 (6300 sh), 332.0 (7500), 421.6 (19100); MS *m/z* (rel intensity) 226 (M$^+$+1; 16), 225 (M$^+$; 100), 223 (13), 197 (11), 196 (16). Found: C, 69.57; H, 3.67; N, 12.23%. Anal. Calcd for C$_{13}$H$_8$N$_2$S: C, 69.61; H, 3.60; N, 12.49%.

24(100%): Orange needles, mp 180—181 °C; ^{1}H NMR δ = 2.44 (3H, d, J = 1.0 Hz), 3.79 (3H, s), 6.45 (1H, q, J = 1.0 Hz), 6.88 (1H, ddd, J = 10.5, 8.0, 1.0 Hz), 6.94 (1H, ddd, J = 12.0, 8.0, 2.0 Hz), 7.38 (1H, m), 7.43 (1H, dm, J = 12.0 Hz); ^{13}C NMR δ = 13.3, 35.1, 64.1, 110.7, 115.8, 117.5, 126.1, 127.8, 128.3, 132.7, 133.2, 134.2, 144.9, 153.2; IR (KBr) 2180 cm^{-1}; *m/z* 221 (M$^+$; 100): Found: C, 75.79; H, 5.04; N, 18.78%. Anal. Calcd for C$_{14}$H$_{11}$N$_3$: C, 75.99; H, 5.01; N, 18.99%.

Type I
8: X=O (ref. 12)
9: X=S (ref. 12)
10: X=NMe (ref. 12)

Type II
11: X=O (ref. 12)
12: X=S (ref. 12)
13: X=NMe (ref.12)

Type III
14: X=OMe (ref. 12)
15: X=SMe (ref. 12)
16: X=NMe$_2$(ref. 12)
17: X=H

18: X=CHMe$_2$
19: Y=CHMe$_2$
20: Z=CHMe$_2$
21: U=CHMe$_2$ (ref. 12)

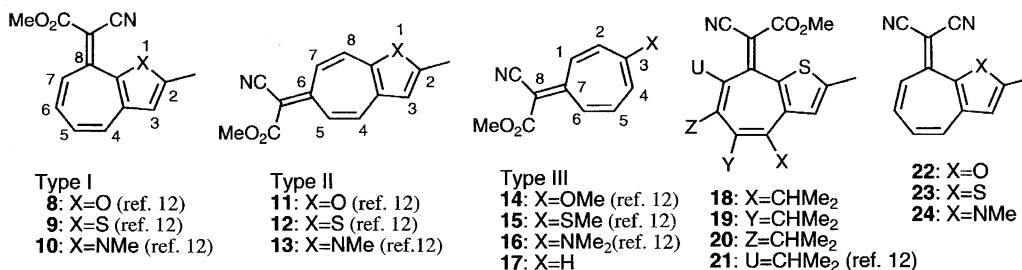**22:** X=O
23: X=S
24: X=NMe

Chart 1. Structures of the push–pull heptafulvenes investigated.

Kinetics. Kinetic analysis was carried out by variable-temperature ^{1}H NMR spectral measurements at 270 MHz in acetonitrile-d_3, N,N-dimethylformamide-d_7, and toluene-d_8. The instrument was a JEOL GSX 270 H spectrometer. There is an instrumental error (between figures on the digital display and the direct readings from the thermocouple set for determination at the hole) as large as up to ± 0.9 °C. Data were collected from the mean values of at least three measurements for each temperature.

Line-Shape Analysis. The rate constants were determined by line-shape analysis of the pronounced signals using the DNMR2 QCPE140 program.$^{14)}$ The temperature ranges were -20 to 100 °C in toluene-d_8, and -40 to 60 °C in acetonitrile-d_3, and -50 to 120 °C in N,N-dimethylformamide-d_7.

Saturation Transfer Method. When the line-shape analysis was not applicable, the saturation transfer method$^{15)}$ was employed to obtain the thermodynamic parameters. For example, the equilibrium constants between **11A** (E-form) and **11B** (Z-form) were calculated from the simultaneous equations.

$$[A] \underset{k_B}{\overset{k_A}{\rightleftharpoons}} [B] \qquad k_A[A] = k_B[B]$$

$$M_A/M_{OA} = 1/(1 + k_A T_{1A}) \qquad 1/T_{1A\text{eff}} = T_{1A} + k_A$$

[A], concentration of isomer **A**; [B], concentration of isomer **B**; M_A/M_{OA}, fraction of remaining magnetization under saturation transfer conditions; $T_{1A\text{eff}}$, observable longitudinal relaxation time; T_{1A}, theoretical longitudinal relaxation time.

The H-7 at $\delta = 7.39$ of the isomer **11A** in N,N-dimethylformamide-d_7 at 90 °C was saturated by irradiation to observe the saturation transfer to the H-7 of **11B** at $\delta = 8.73$. The value of M_B/M_{OB} was obtained by comparison of the steady-state intensity with a resultant saturating field and a nonsaturating field where the temperature was measured. The ratio of **A** and **B** is $1 : 1.14$. Then, the value of M_B/M_{OB} is 0.55. The value of $T_{1B\text{eff}}$ (3.33 s) was observed from DBHMG pulse sequence. The activation parameters were obtained by a linear least square plot of $\ln k$ vs. $1/T$ according to the Eyring equation.

Results and Discussion

The NMR Spectroscopic Analyses of Isomers. At -40 °C, the ^{1}H NMR spectrum of **9** in acetonitrile-d_3 showed two sharp doublet signals at $\delta = 8.46$ ($J = 12.1$ Hz) and at $\delta = 7.42$ ($J = 12.0$ Hz), which were assigned to H-7.$^{16)}$ The ratio was $91 : 9$. This implies the existence of two rotational isomers. From a consideration of the magnetic anisotropy of a methoxycarbonyl group, the major isomer with a signal at $\delta = 8.46$ is assigned to be **9A** and the other is **9B**. The smaller cyano group is located at an inner side of the major **9A**. In acetonitrile-d_3 at 60 °C, **9** showed a broad and coalesced signal with a half-height width of 46 Hz.

The ^{1}H NMR spectrum of **9** in chloroform-d at room temperature showed a broad doublet ($J = 12.0$ Hz) at $\delta = 8.48$, which was assigned to H-7 of **9A**. The doublet of **9B**, however, was not observed because of the overlap with other signals. At 60 °C, the signal of H-7 of **9A** was still a broad doublet at $\delta = 8.40$ ($J = 11.3$ Hz) and did not coalesce in chloroform-d. The signal of **9B** was again undetectable. Similarly, the ^{1}H NMR spectrum of **9** in N,N-dimethylformamide-d_7 at -50 °C showed a sharp doublet ($J = 12.1$ Hz) at $\delta = 8.58$ and another at $\delta = 7.54$. The radio was $90 : 10$ and the major isomer was **9A**.

The ^{1}H NMR spectrum of **10** showed broad signals at room temperature in acetonitrile-d_3. At -40 °C, it showed two rotational isomers **10A** ($\delta = 8.75$, d, $J = 11.7$ Hz, H-7) and **10B** ($\delta = 7.62$, d, $J = 12.1$ Hz, H-7) with a ratio of $30 : 70$. The bulkier substituent, the methoxycarbonyl group, of the major **10B** is located at the inner side of the molecule. The structures of **10A** and **10B** were assigned from the NMR data that the chemical shift of H-7 of 8-(dicyanomethylidene)-1,2-dimethyl-8H-cyclohepta[b]pyrrole (**24**) is $J = 7.43$ (dm, $\delta = 12.0$ Hz). At 60 °C, the broad doublet signal of H-7 appeared at $\delta = 7.95$. The ^{1}H NMR spectrum of **10** in N,N-dimethylformamide-d_7 at -50 °C showed the presence of **10A** ($\delta = 8.84$, d, $J = 12.5$ Hz, H-7) and **10B** ($\delta = 7.70$, d, $J = 12.5$ Hz, H-7) with a ratio of $34 : 66$. Again, the more hindered **10B** was the major isomer. However, **10A** ($\delta = 9.09$, d, $\delta = 12.5$ Hz, H-7) becomes the major isomer with a ratio of $55 : 45$ at -20 °C in the least polar solvent examined, toluene-d_8.

The ^{1}H NMR spectrum of **8** in acetonitrile-d_3 at 27 °C showed sharp signals of H-7 at $\delta = 8.92$ (d, $J = 12.8$ Hz) and $J = 7.42$ (dd, $J = 12.8$, 1.0 Hz) of two rotational isomers **8A** and **8B** in a ratio of $92 : 8$. At 60 °C, there are still two doublets at $\delta = 8.85$ ($J = 12.8$ Hz) and $\delta = 7.23$ ($J = 11.4$ Hz). Thus, up to 60 °C, the rotation about the C=C bond was not measurable by the line-shape-analysis. In N,N-dimethylformamide-d_7, two sharp methyl signals at $\delta = 2.57$ (d, $J = 1.1$ Hz) and 2.48 (d, $J = 1.1$ Hz) at 20 °C were observed in the ratio of $91 : 9$.

In the less hindered Type II heptafulvenes and the monocyclic Type III derivatives, the relative populations of the isomers **A** (E-isomer) and **B** (Z-isomer) were nearly $1 : 1$ ($47 : 53$ to $50 : 50$) in N,N-dimethylformamide-d_7. The geometrical isomers **A** and **B** of **11**, **12**, and **13** were assigned from the ^{1}H NMR decoupling and NOE experiments. Namely, among five aromatic proton signals of **11A**, at $\delta = 6.39$ (1H, s), 7.28 (1H, d, $J = 12.1$ Hz), 7.35 (1H, d, $J = 12.1$ Hz), 7.53 (1H, dd, $J = 12.1$, 2.2 Hz), and 8.85 (1H, dd, $J = 12.1$, 2.2 Hz), and another **11B**, at $\delta = 6.39$ (1H, s), 7.25 (1H, d, $J = 12.1$ Hz), 7.32 (1H, d, $J = 12.5$ Hz), 7.47 (1H, d, $J = 12.1$, 2.2 Hz), and 8.86 (1H, br d, $J = 12.5$ Hz),$^{11)}$ easily identifiable H-5 (8.85) and H-7 (7.53) signals (**11A**) and H-5 (7.47) and H-7 (8.86) (**11B**),$^{13)}$ were mutually spin-coupled with C-4 (7.28) and C-8 (7.35) (**11A**) and C-4 (7.25) and C-8 (7.32) (**11B**), respectively. The same was true in the cases of **12** and **13**. In addition, there are two methyl singlets in **13** in N,N-dimethylformamide-d_7; an exhibition of NOE (18%) with H-8 signal identified the signal at $\delta = 3.91$ to be the N-methyl, and the other, at $\delta = 3.74$, to be the O-methyl signal. All these observations distinguished the geometrical isomerism as depicted.

Similarly, the geometrical isomers **A** and **B** of monocyclic Type III derivatives (**14**, **15**, and **16**) were assigned on the basis of the chemical shift and the coupling constant criteria.$^{12)}$

Configuration of the Major Isomer. Table 1 summarizes the populations of isomers **A** and **B** of Type I compounds (**8**, **9**, and **10**) in the three solvents. For compounds **8** and **9**, the relative populations of **A/B** were not much different for various solvents, but for **10**, the populations varied according

1322 *Bull. Chem. Soc. Jpn., 69, No. 5 (1996)*

Geometrical Isomerism of Heptafulvenes

Table 1.   Kinetic Parameters for Isomerizations (Changes from the Major to the Minor Isomers)

Compd	A/B	(t/°C)	$\Delta H^{\ddagger}$/kJ mol⁻¹	$\Delta S^{\ddagger}$/kJ mol⁻¹ K⁻¹	$\Delta G^{\ddagger}$/kJ mol⁻¹ᵃ⁾	Solvent	Methodᵇ⁾
8	91/9	(20)	60.8± 1.8	−64.3± 5.3	79.9± 0.3	DMF-d_7	TLA
9	91/9	(40)	43.3± 1.1	−110.0± 3.1	76.1± 0.2	MePh-d_8	TLA
	91/9	(−40)	39.6± 2.2	−78.3± 7.6	62.9± 0.3	MeCN-d_3	TLA
	90/10	(−50)	35.7± 1.1	−93.0± 3.9	63.4± 0.2	DMF-d_7	TLA
10	55/45	(−20)	38.2± 1.4	−91.4± 4.8	65.4± 0.1	MePh-d_8	TLA
	30/70	(−40)	39.7± 0.9	−47.1± 3.4	53.7± 0.1	MeCN-d_3	TLAᶜ⁾
	34/66	(−50)	39.3± 1.0	−57.1± 3.9	56.3± 0.2	DMF-d_7	TLA
18	88/12	(−40)	40.5± 0.9	−63.7± 3.2	59.5± 0.1	MeCN-d_3	TLA
19	91/9	(−40)	41.5± 1.0	−65.8± 3.5	61.1± 0.1	MeCN-d_3	TLA
20	91/9	(−39)	38.9± 2.5	−68.9± 8.9	59.5± 0.3	MeCN-d_3	TLA
11	47/53	(60)	62.8± 3.3	−90.6± 9.3	89.8± 0.6	DMF-d_7	ST
12	47/53	(95)	79.5± 2.4	−64.3± 6.3	98.6± 0.5	DMF-d_7	STᶜ⁾
13	48/52	(40)	57.7± 2.5	−67.4± 7.4	77.8± 0.3	DMF-d_7	TLA
14	47/53	(70)	· 62.4± 4.5	−93.1± 12.4	90.2± 0.8	DMF-d_7	ST
15	50/50	(90)	80.4± 7.8	−57.2± 20.8	97.5± 1.6	MePh-d_8	ST
16	50/50	(−10)	54.9± 1.9	−44.7± 5.6	68.3± 0.3	MePh-d_8	TLA

a) at 25 °C; b) TLA=total line-shape analysis, ST=saturation transfer; c) changes for minor to major isomers.

to the polarity of the media; in less polar solvent (toluene-d_8), A was the major isomer (55/45) and in more polar solvents (acetonitrile-d_3 and N,N-dimethylformamide-d_7), B was the major one (30/70 and 34/64). Geometrical isomers **8A** and **9A**, in which the methoxycarbonyl groups are on the outer side of the molecule, are dominant for steric reasons. However, the major isomer of **10** (**10B**) has a methoxycarbonyl group in the more hindered inner side of the molecule in polar solvents, such as N,N-dimethylformamide-d_7 and acetonitrile-d_3. A similar observation has been reported for **6**; **6A**, having the cis-relationship between the bulky methoxycarbonyl and the dimethylamino groups, is the major isomer in chloroform-d.[8] It is clear that the trigonal methoxycarbonyl group is bulkier than the linear cyano group. However, for the sterically crowded **10** we should take another factor into account; since the nitrogen carries the methyl group, the linear cyano group on the semicyclic β-carbon has no means of reducing the steric hindrance, but the methoxycarbonyl group on that carbon should be capable by changing a conformation (a gear effect). This was parallel to the MNDO-calculated dipole moments (μ) of compounds **8**, **9**, and **10** (vide infra). In the polarized form of **10A**, the sp²-hybridized nitrogen should extend the methyl group within the plane of the five-membered heterocycle, and this is disfavored by the presence of the linear cyano group. As the result, the dipole moment was exceptionally small and the difference ($\Delta\mu$) between A and B forms was large.

Dynamic NMR Spectral Measurements.   The rotational barriers of **8**, **9**, and **10** were determined by the complete line-shape analysis of the variable-temperature ¹H NMR spectra (270 MHz) in the range of −40 to 60 °C in acetonitrile-d_3 and −50 to 120 °C in N,N-dimethylformamide-d_7, comparing with the simulated spectra.[14] Those of **13** were determined by ¹H NMR spectroscopy (500 MHz) in the temperature range between 30 and 100 °C in N,N-dimethylformamide-d_7. The rates for **11**, **12**, **14**, and **15** were determined by the saturation transfer method, since their NMR

spectral changes were not sufficient for the complete line-shape analysis even at 120 °C in N,N-dimethylformamide-d_7. Figure 1 shows the ¹H NMR spectrum of **11** together with its saturation transfer experiment, which indicates an inverted signal enhancement of H-7 of isomer **11B** by irradiation of the signal of H-7 of isomer **11A**. The consistency of the results from the two methods was assured by comparison with the data obtained from **13**; at 30 °C in N,N-dimethylformamide-d_7, the rotational barriers were 77.5 kJ mol⁻¹ (saturation transfer method) and 77.8 kJ mol⁻¹ (line-shape analysis), respectively, which are within experimental error.
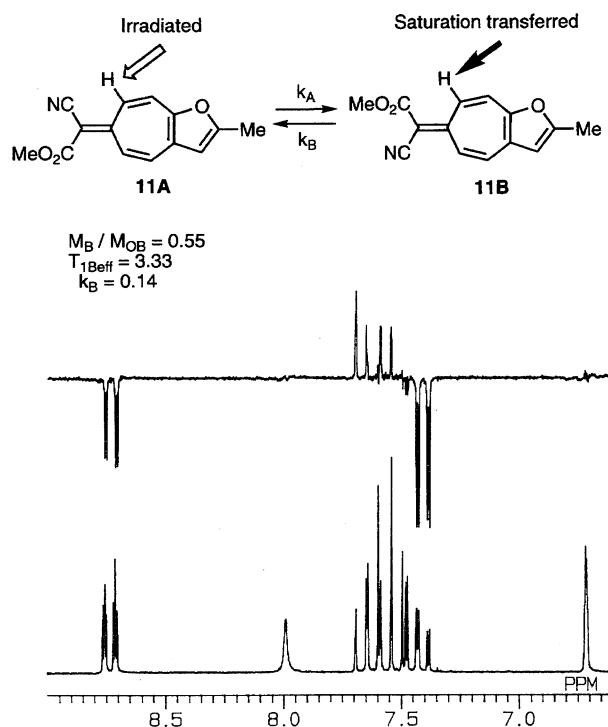
Fig. 1.   The ¹H NMR spectrum of compound **11** in DMF-d_7 at 90 °C.

The activation parameters are also included in Table 1.

Table 1 shows that the C=C barriers decrease in the sequence of **8>9>10**, i.e., the barrier-lowering effect of the heteroatom increases in the sequence, N>S>O. The activation enthalpies ($\Delta H^{\ddagger}$) of **10** and **9** are almost the same (39.7 kJ mol^{-1} for **10** and 39.6 kJ mol^{-1} for **9** in acetonitrile-d_3 and 39.3 kJ mol^{-1} for **10** and 35.7 kJ mol^{-1} for **9** in *N,N*-dimethylformamide-d_7). However, **8** has a quite large $\Delta H^{\ddagger}$ value (60.8 kJ mol^{-1}) in *N,N*-dimethylformamide-d_7. The large negative $\Delta S^{\ddagger}$ values in unimolecular reactions indicate a charge-separated transition state,[4,17,18] and in the present case, the delocalization of the positive charge is favored by contribution of the aromatic $(4n+2)\pi$ system (Chart 2).

The rates on **10** and **9** in toluene-d_8 were determined in the temperature range from -20 to 100 °C; the $\Delta G^{\ddagger}$ values were larger than those in *N,N*-dimethylformamide-d_7 and in acetonitrile-d_3. Although the $\Delta H^{\ddagger}$ values did not change, the larger negative $\Delta S^{\ddagger}$ values were observed in toluene-d_8, which caused the largest $\Delta G^{\ddagger}$ value for **9** and **10**. It has been pointed out[19] that the entropy changes are larger in a nonpolar solvent since unordered molecules in the ground state will take a larger loss of entropy upon solvation in the reaction of uncharged species to form ions. This should be the present

case. In nonpolar toluene-d_8, molecules are unordered in the ground state. In the transition state, the incipient charge-separated molecules could be solvated more tightly by toluene-d_8 through the interaction between the charge-separated heptafulvenes and toluene-d_8 via π–π stacking. The isopropyl derivatives, **18—20**, of **9** behaved quite similarly.

As can be seen in Table 1, the most crowded **10** has the lowest rotational barrier in the hindered series. Certainly, the steric repulsion is expected to twist the C=C bond to increase the ground state energy and to make the rotational barrier lower.[20] In order to clarify the steric acceleration of the rotation, we measured the rate of less hindered Type II isomers, **11—13**, with a heterocycle at the remote position.

The less hindered Type II compounds (**11**, **12**, and **13**) have higher $\Delta H^{\ddagger}$ and $\Delta G^{\ddagger}$ values than the hindered Type I compounds (**8**, **9**, and **10**). The barriers follow the order N<S<O for Type I compounds and the order N<O<S for Type II compounds and also for the monocyclic compounds (**14**, **15**, and **16**).

Estimation of Bond Polarization from the ^{13}C Chemical Shifts. At first, the ^{13}C NMR chemical shifts of the β-carbons of the exocyclic C=C, δ(C-β), of push–pull ethylenes should be a good measure of bond polarization. The uncondensed parent 8-cyano-8-methoxycarbonylheptafulvene (**17**) revealed some polarized character for the exocyclic C=C bond as its δ(C-α), δ(C-β), and the difference $\Delta\delta$, are 161.6, 89.8, and 71.8. Table 2 summarizes the ^{13}C NMR chemical shifts of the related signals of the heptafulvenes in chloroform-d. By condensation of a heterocycle to form the Type I derivatives, the electron density of the heptafulvene system was increased to make the chemical shifts higher in the order of N>S>O for the δ(C-α), and as the result, in-
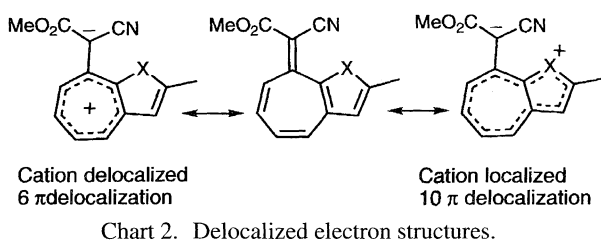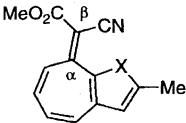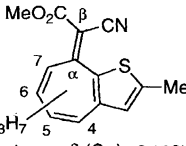

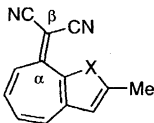Cation delocalized
6 πdelocalization

Cation localized
10 π delocalization

Chart 2. Delocalized electron structures.
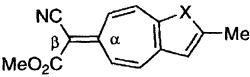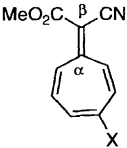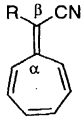
Table 2. The ^{13}C NMR Chemical Shifts and Their Differences of the Exocyclic C=C in CDCl$_3$

Compound	δ (Cα)	δ (Cβ)	$\Delta\delta$
8 (X = O)	158.5	81.7	76.8
9 (X = S)	156.6	89.0	67.6
10 (X = NMe)	151.7	85.5	66.2

Compound	δ (Cα)	δ (Cβ)	$\Delta\delta$
18 (C$_3$H$_7$ at 4)		90.1	
19 (C$_3$H$_7$ at 5)		87.4	
20 (C$_3$H$_7$ at 6)		87.8	
21 (C$_3$H$_7$ at 7)		101.3	

Compound	δ (Cα)	δ (Cβ)	$\Delta\delta$
22 (X = O)	159.9	61.5	98.3
23 (X = S)	157.0	66.5	90.5
24 (X = NMe)	153.2	64.1	89.1

Compound	δ (Cα)	δ (Cβ)	$\Delta\delta$
11 (X = O)	160.2	88.0	72.2 (**A**)
	160.0	88.0	72.0 (**B**)
12 (X = S)	160.2	89.5	70.7 (**A**)
	160.1	89.5	70.6 (**B**)
13 (X = NMe)	160.2	83.0	77.2 (**A**)
	160.3	82.9	77.4 (**B**)

Compound	δ (Cα)	δ (Cβ)	$\Delta\delta$
14 (X = OMe)	159.8	87.5	72.3 (**A**)
	160.0	87.5	72.5 (**B**)
15 (X = SMe)	160.4	89.0	71.4 (**A**)
	160.4	89.0	71.4 (**B**)
16 (X = NMe$_2$)	159.0	79.2	79.8 (**A**)
	157.4	79.2	78.2 (**B**)

Compound	δ (Cα)	δ (Cβ)	$\Delta\delta$
1 (R = CN)	163.7	70.1	93.6
17 (R = CO$_2$Me)	161.6	89.8	71.8

creased electron density at the C-β caused a high-field shift for the δ(C-β) in the order of O>N>S. The difference of chemical shifts for the exocyclic carbon signals, $\Delta\delta$, was in the order of N>S>O. On the other hand, in the less hindered Type II heptafulvenes (11, 12, and 13) and the monocyclic Type III series (14, 15, and 16), the magnitudes of the high-field shifts for the δ(C-β) were the largest with the nitrogen derivatives 13 and 16; they are N>O>S, being consistent with the observed order for the ease of rotations in Types II and III.

In Type I series, the steric repulsion should raise the energy of the ground state to facilitate the rotation, and this must be predominant in the N-methylpyrrole derivative. Furthermore, the pyrrole should stabilize the transition state, since its π donating ability is better than those of furans and thiophenes. As the results, the barrier of 10 becomes the smallest.

Consequently, in the hindered Type I heptafulvenes, the steric effect certainly destabilizes the ground states, and the electronic effect stabilizes the transition states. In the less hindered Type II and the monocyclic Type III series, the rotational barriers obeyed the electron donating ability, as in the order: N>O>S.

Next, it was observed that the δ(C-β) of 21 (101.3) is lower than those of 9 (89.0) and other isopropyl derivatives, 18 (90.1), 19 (87.4), and 20 (87.8). This should again indicate the significance of the steric effect; the seven-membered ring of 21 should be forced to bend more than the others to reduce steric repulsions by the isopropyl group. The exocyclic C=C bond of 21 should have more double bond character than

those of 18—20. The UV spectrum [λ_{max} 240 nm (ε 12900 sh), 294 (6900), 396 (6900)] of 21, which was also markedly different form those of the other isomers, suggested that the seven-membered ring of 21 is in a boat from similar to the ring of 8,8-dicyano-1,6-dimethylheptafulvene (2)[2] to diminish the conjugation; the parent compound 9 and other derivatives 18—20 with an isopropyl group at the less hindered position had the longest absorption maxima at 418—430 nm with the stronger absorption coefficients (ε 10800—17500).

In the case of the dicyanomethylidene derivatives, such as 8-(dicyanomethylidene)-1,2-dimethyl-8H-cyclohepta[b]-pyrrole (24), the chemical shift differences between the two cyano groups were small. In addition, the intensity of the signals was too weak for line-shape analysis.

MO Calculations. The semiempirical MNDO-PM3 calculation was applied to 8, 9, 10, 11, 12, 13, and 16. Geometries were optimized to give minimum heats of formation. The figures can be seen in Table 3, summarized together with the calculated dipole moments.

As representative results, the conformations, with calculated structural parameters, at the ground states and the transition states of 8 (8A, 8B, and 8T) and 10 (10A, 10B, and 10T) are illustrated in Fig. 2. Table 4 summarizes the dihedral angles of the ground and the transition states (Tables 5 and 6). In the hindered series (8, 9, and 10), the dihedral angles (C-6–C-7–C-8–C-9) of 10 (128.8°) and 9A (125.2°) are smaller than that (141.4°) of 8A. In the less hindered series (11A, 12A, and 13A) and the monocyclic 16A, the corresponding dihedral angles are 135.5—139°. Therefore,

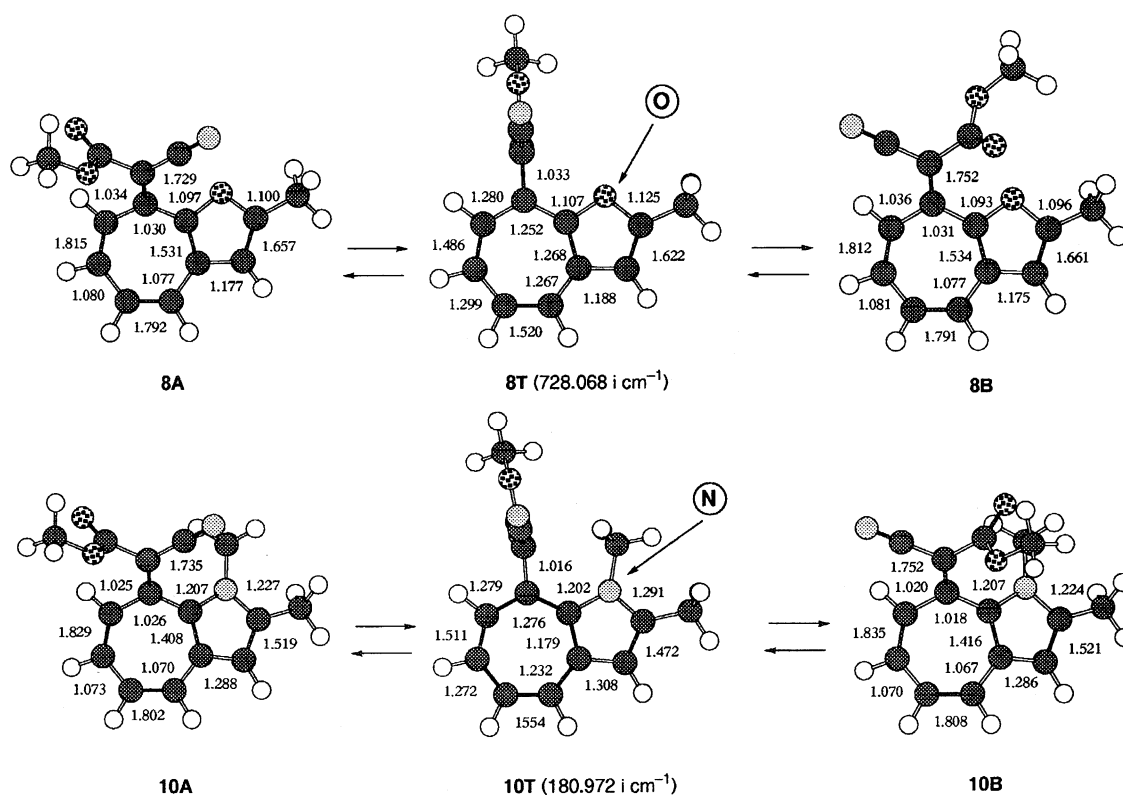Fig. 2. The calculated bond orders (MNDO-PM3) for rotatomers A and B and their transition states of 8 and 10.

Y. Ikeda et al.

Bull. Chem. Soc. Jpn., 69, No. 5 (1996) 1325

Table 3. Calculated Heats of Formation and Dipole Moment of Type I Compounds by MNDO-PM3

Compd	ΔH/kJ mol^{-1}		μ/Debye	
	A	B	A	B
8	−28.12	−27.54	4.43	4.95
9	132.54	135.94	4.56	4.50
10	83.58	86.83	2.98	4.23
11	−39.52	−39.54	5.38	5.18
12	116.84	116.67	4.99	4.49
13	71.29	71.91	6.43	7.40
16	15.18	15.26	4.59	5.01

Table 4. Optimized Dihedral Angles[a] of Type I Compounds by MNDO-PM3

Compd	Angles		
	Ground state/°		Transition state/°
	A	B	
8	141.4	142.4	178.8
9	125.2	123.6	—
10	128.8	125.3	177.5
11	138.9	138.6	177.9
12	135.7	135.4	178.5
13	138.3	138.2	179.0
16	135.5	135.5	177.0

a) Defined as the angles of two planes formed by each carbon on semicyclic C=C and the two adjacent carbons.

it may be concluded that **10** and **9** are bent to more extent and are more sterically hindered in the ground state. This is consistent with **10** and **9** having the low values of $\Delta H^{\ddagger}$, which imply the destabilization of the ground state. The bond order of the exocyclic C=C bond in the ground state showed that the exocyclic C=C bond of **8** has the highest single bond character and that **8** has the most planar conformation. This is in accordance with the conclusion observed from the chemical shift difference of the exocyclic C=C carbons. Therefore, the ground state of **8** is more stable than those of **9** and **10**.

On the other hand, the dihedral angles in the transition states of **8** and **10** are 177—179°. The substituents on the

exocyclic C=C bond are nearly orthogonal to the plane of the seven-membered ring. The bond order of the exocyclic C=C bond decreased on going to the transition state. At the same time, the bond alternation of seven-membered rings was reduced. However, the bond orders of the hetero rings slightly changed. These results reveal that a cycloheptatrienylium cation structure contributed in the transition state and that the electronic effect rather than the steric effect became more important in the transition state. The electron donating ability of these elements follows the order N>O>S, which follows the

Table 5. Z-Matrix of Transition State (**8**)

Atom number (I)	Chemical symbol	Bond length (Ångstroms) NA : I	Bond angle (Degrees) NB : NA : I	Twist angle (Degrees) NC : NB : NA : I	NA	NB	NC
1	C(1)						
2	C(2)	1.40904			1		
3	C(3)	1.42351	132.32684		2	1	
4	C(4)	1.39757	128.76492	−0.10067	3	2	1
5	C(5)	1.37219	126.42831	−0.17908	4	3	2
6	C(6)	1.40091	128.95986	−0.00411	5	4	3
7	C(7)	1.37610	130.52424	0.05961	6	5	4
8	C(8)	1.44369	119.96562	−178.88741	1	2	3
9	C(9)	1.43032	118.55179	89.85750	8	1	2
10	O(10)	1.38652	118.85963	179.65315	2	1	3
11	O(11)	1.23456	126.72483	−0.60307	9	8	1
12	C(12)	1.43999	106.11553	179.67315	3	2	1
13	H(13)	1.10093	115.66691	179.69578	4	3	2
14	C(14)	1.39307	117.46970	−90.24171	8	1	2
15	H(15)	1.10141	115.90949	179.86132	5	4	3
16	H(16)	1.08826	125.81479	−179.88414	12	3	2
17	H(17)	1.10249	114.35985	179.87263	6	5	4
18	C(18)	1.37730	106.59426	−0.02056	12	3	2
19	H(19)	1.10511	116.05363	179.62145	7	6	5
20	C(20)	1.47246	131.51422	179.98314	18	12	3
21	H(21)	1.09723	110.49561	1.11592	20	18	12
22	H(23)	1.09960	111.12412	−119.01410	20	18	12
23	H(24)	1.09959	111.17602	121.29173	20	18	12
24	N(28)	1.16693	178.59870	1.74412	14	8	1
25	O(29)	1.37684	115.14130	179.29204	9	8	1
26	C(32)	1.40792	117.95938	−179.63473	25	9	8
27	H(33)	1.09320	102.47966	179.71609	26	25	9
28	H(34)	1.09541	112.17882	61.49610	26	25	9
29	H(35)	1.09542	112.13522	−62.07861	26	25	9

Table 6. Z-Matrix of Transition State (**10**)

Atom number (I)	Chemical symbol	Bond length (Ångstroms) NA : I	Bond angle (Degrees) NB : NA : I	Twist angle (Degrees) NC : NB : NA : I	NA	NB	NC
1	C(1)						
2	C(2)	1.40801			1		
3	C(3)	1.44159	128.62735		2	1	
4	C(4)	1.40395	129.77679	1.92959	3	2	1
5	C(5)	1.36623	127.70445	1.06132	4	3	2
6	C(6)	1.40234	128.12200	−0.74963	5	4	3
7	C(7)	1.37119	129.80268	−1.46885	6	5	4
8	C(8)	1.45293	120.40118	175.70589	1	2	3
9	C(9)	1.43030	119.27477	95.06251	8	1	2
10	N(10)	1.42007	125.59237	−178.49595	2	1	3
11	O(11)	1.23414	127.08646	−8.50729	9	8	1
12	C(12)	1.41950	107.88150	−178.33753	3	2	1
13	H(13)	1.10146	114.93132	−179.46161	4	3	2
14	C(14)	1.39483	116.76408	−93.49478	8	1	2
15	H(15)	1.10061	116.45752	179.18456	5	4	3
16	H(16)	1.08941	125.75334	179.76155	12	3	2
17	H(17)	1.10191	114.67777	179.14341	6	5	4
18	C(18)	1.39266	108.34029	−0.45410	12	3	2
19	H(19)	1.10503	115.42546	−178.91004	7	6	5
20	C(20)	1.47707	125.99733	−179.69318	18	12	3
21	H(21)	1.09810	110.26563	−0.13753	20	18	12
22	C(22)	1.46606	127.31679	−2.86977	10	2	1
23	H(23)	1.09983	111.70083	−119.68534	20	18	12
24	H(24)	1.09975	111.69822	119.42103	20	18	12
25	H(25)	1.09866	110.76400	178.46594	22	10	2
26	H(26)	1.10264	110.65293	57.77821	22	10	2
27	H(27)	1.10221	110.45704	−60.95779	22	10	2
28	N(28)	1.16711	178.55396	39.48979	14	8	1
29	O(29)	1.37847	115.00454	172.99599	9	8	1
30	C(32)	1.40786	118.04876	−179.98924	29	9	8
31	H(33)	1.09317	102.46789	179.21587	30	29	9
32	H(34)	1.09531	112.21405	60.95112	30	29	9
33	H(35)	1.09545	112.07056	−62.62001	30	29	9

σ_p^+ value of these three elements.[21] Therefore, the transition state energy of **10** is the lowest.

In the less hindered Type II and the monocyclic Type III, the barrier increased in the order N<O<S. The dihedral angles are 135.5—139° in the ground state and 177—179° in the transition state. The electron donating ability of the hetero atoms affects the energy states much more effectively in *more planar transition state* than in *less planar ground state*.

It is interesting to note that the dipolar contribution is responsible for the observed predominance of the **10B** isomer over **10A** isomer in the polar solvents. In the sterically-hindered Type I compounds, isomers **A** are shown to be more stable than isomers **B**. In cases of **8** and **9**, the calculated dipole moments of respective isomers **8A** and **8B** and **9A** and **9B** are similar to each other, while isomer **10B** has a larger dipole moment than isomer **10A**. Thus, the dipolar effect favored the contribution of the more hindered polar form (isomer **10B**) in polar solvents.

Conclusion.   Apparently, the order of facilitated internal rotations of the hindered Type I compounds was O<S<N, being the same as that of compounds **4**.[4] On the other hand,

in the less hindered Type II series, the barriers of rotation are in the decreasing order N>O>S, in contrast to compounds **4**. The transition state of **4** could achieve the 6π-delocalized contribution by involvement only of the unshared electron pair of the hetero atoms, generating localized positive charge on the hetero atoms.[4] Contrastingly, throughout Types I—III series, such 6π-delocalizations should be achieved solely by the delocalization of seven-membered π-electron systems, and the hetero atoms played a role in further stabilization of expanded 10π-delocalization at the expense of charge localization on the heteroatoms in the transition state. Therefore, the different order in the isomerization of Types I and II should mainly be due to the steric factor.

The $\Delta H^{\ddagger}$ value for **9** was smaller than that of **8**. The $\Delta H^{\ddagger}$ values for **12** and **15** were the largest among the less hindered Type II and monocyclic Type III series. This unusually low $\Delta H^{\ddagger}$ value of **9** reflects the destabilization of the ground state due to repulsive steric interactions. And, from the kinetic analyses with the heptafulvene derivatives carrying different types of hetero atom substituents, we conclude that the delocalization of the unshared electron pairs of hetero atoms played an additional role for the rotation

of the exocyclic C=C of the heptafulvenes via the polarized transition state.

References

1) H. Shimanouchi, T. Ashida, Y. Sasada, M. Kakudo, I. Murata, and Y. Kitahara, *Bull. Chem. Soc. Jpn.*, **39**, 2322 (1966).

2) H. Shimanouchi, Y. Sasada, C. Kabuto, and Y. Kitahara, *Tetrahedron Lett.*, **1968**, 5053.

3) B. Z. Yin, A. Mori, H. Takeshita, and H. Inoue, *Chem. Lett.*, **1991**, 1011.

4) I. Belsky, H. Dodiuk, and Y. Shvo, *J. Org. Chem.*, **24**, 2734 (1977).

5) The geomerical isomers, **A** and **B**, were defined on the basis of the *E-* /*Z*-relationship.

6) D. Adhikesavalu and K. Venkatesan, *Acta Crystallogr.*, *Sect. C*, **C39**, 589 (1983).

7) J. Sandström and I. Wennerbeck, *Acta Chem. Scand. Ser. B*, **32**, 421 (1978).

8) Y. Shvo and I. Belsky, *Tetrahedron*, **25**, 4649 (1969).

9) Y. Shvo and H. Shanan-Atidi, *J. Am. Chem. Soc.*, **91**, 6683 and 6689 (1969).

10) Y. Ikeda, B. Z. Yin, N. Kato, A. Mori, and H. Takeshita, *Chem. Lett.*, **1992**, 1453.

11) Y. Ikeda, B. Z. Yin, N. Kato, A. Mori, and H. Takeshita, *Heterocycles*, **36**, 1725 (1993).

12) Y. Ikeda, B. Z. Yin, A. Mori, and H. Takeshita, *Kyushu Daigaku Sogo Rikogaku Kenkyuka Hokoku*, **16**, 295 (1994).

13) H. Takeshita, K. Uchida, and H. Mametsuka, *Heterocycles*, **20**, 1709 (1983).

14) G. Binsch and D. A. Kleier, *QCPE*140.

15) D. G. Gadiar, "Nuclear Magnetic Resonance and Its Applications to Living Systems," Oxford University Press, New York (1982); H. Cho, T. Iwasaki, M. Ueda, A. Mizuno, K. Mizukawa, and M. Hamaguchi, *J. Am. Chem. Soc.*, **110**, 4832 (1988).

16) Assignment of H-5 and H-7 was unambiguous; i.e., the α-proton signals to the semicyclic C=C appeared at δ =7.43 (for dicyano derivative **22**), 7.47 (for **8B**), and 8.97 (for **8A**).

17) U. Berg and U. Sjöstrand, *Org. Mag. Reson.*, **11**, 555 (1978).

18) D. E. Gallis, J. A. Warshaw, B. J. Acken, and D. R. Crist, *J. Org. Chem.*, **56**, 6352 (1991).

19) H. E. Cox, *J. Chem. Soc.*, **1921**, 142; R. G. Pearson, *J. Chem. Phys.*, **20**, 1478 (1952).

20) I. R. Gault, W. D. Ollis, and I. O. Sutherland, *J. Chem. Soc., Chem. Commun.*, **1970**, 269; I. Agranat, M. Rabinovitz, A. Weitzen-Dagan, and I. Gosnay, *J. Chem. Soc., Chem. Commun.*, **1972**, 732; M. Rabinovitz, I. Agranat, and A. Weitzen-Dagan, *Tetrahedron Lett.*, **1974**, 1241.

21) O. Exner, "Advances in Linear Free Energy Relationship," ed by N. B. Chapman and J. Shorter, Plenum, New York (1972), pp. 28—32.